PHILOSOPHICAL TRANSACTIONS A

rsta.royalsocietypublishing.org

Research

Cite this article: Mizus II, Kyuberis AA, Zobov NF, Makhnev VYu, Polyansky OL, Tennyson J. 2018 High-accuracy water potential energy surface for the calculation of infrared spectra. *Phil. Trans. R. Soc. A* **376**: 20170149.
http://dx.doi.org/10.1098/rsta.2017.0149

Accepted: 30 November 2017

One contribution of 14 to a theme issue 'Modern theoretical chemistry'.

Subject Areas:
chemical physics, computational chemistry, spectroscopy

Keywords:
potential energy surfaces, transition intensities, vibration–rotation

Author for correspondence:
Jonathan Tennyson
e-mail: j.tennyson@ucl.ac.uk

Electronic supplementary material is available online at http://dx.doi.org/10.6084/m9.figshare.c.3969000.

THE ROYAL SOCIETY PUBLISHING

High-accuracy water potential energy surface for the calculation of infrared spectra

Irina I. Mizus[1], Aleksandra A. Kyuberis[1], Nikolai F. Zobov[1], Vladimir Yu. Makhnev[1], Oleg L. Polyansky[2] and Jonathan Tennyson[2]

[1]Institute of Applied Physics, Russian Academy of Science, Ulyanov Street 46, Nizhny Novgorod 603950, Russia
[2]Department of Physics and Astronomy, University College London, Gower Street, London WC1E 6BT, UK

JT, 0000-0002-4994-5238

Transition intensities for small molecules such as water and CO_2 can now be computed with such high accuracy that they are being used to systematically replace measurements in standard databases. These calculations use high-accuracy *ab initio* dipole moment surfaces and wave functions from spectroscopically determined potential energy surfaces (PESs). Here, an extra high-accuracy PES of the water molecule ($H_2{}^{16}O$) is produced starting from an *ab initio* PES which is then refined to empirical rovibrational energy levels. Variational nuclear motion calculations using this PES reproduce the fitted energy levels with a standard deviation of $0.011\,cm^{-1}$, approximately three times their stated uncertainty. The use of wave functions computed with this refined PES is found to improve the predicted transition intensities for selected (problematic) transitions. A new room temperature line list for $H_2{}^{16}O$ is presented. It is suggested that the associated set of line intensities is the most accurate available to date for this species.

This article is part of the theme issue 'Modern theoretical chemistry'.

1. Introduction

Most processes in chemical physics are governed by potential energy surfaces (PESs) and access to accurate PESs, therefore, allows the accurate prediction of properties. In a series of papers, Murrell and co-workers

developed analytic methods of representing PESs for small (usually triatomic) molecules [1–7]. Surfaces predicted on the basis of *ab initio* electronic structure calculations were usually improved by the comparison with or fitting to spectroscopic data. This is precisely the technique we employ here. Much of this work on PESs is captured in the book *Molecular Potential Energy Functions* by Murrell *et al.* [8].

Water molecule is the number one molecule in the HITRAN database [9], which reflects its importance in the Earth's atmosphere, and is a key constituent of other solar system bodies, exoplanets and cool stars [10]. It is, therefore, unsurprizing that Sorbie & Murrell [1], in their seminal paper on constructing PESs, chose to concentrate on water. Many other groups have subsequently followed their lead in constructing accurate semi-empirical PESs for water [11–16], the current authors included [17–22]. An important aspect of the study of the water molecule and the use of the results of these studies in the modelling of different terrestrial and astrophysical environments is the ability to accurately predict line intensities.

Over the last two decades, significant improvements have been made in the accuracy of the water PESs; residuals in predicted rotation–vibration line positions have dropped from approximately $0.6\,\mathrm{cm}^{-1}$ [17,18] to $0.025\,\mathrm{cm}^{-1}$ [15,21]. However, still this figure is about an order-of-magnitude larger than the uncertainty in empirical determinations of rotation–vibration energy levels [23,24]. Improving these predictions towards experimental accuracy places high significance on every step of the calculation. As demonstrated below, these improvements are important not only for accurately reproducing line positions but also for the generation of accurate wave functions for use in intensity calculations.

A testimony to the improvement in the accuracy of computed infrared transition intensities based on the use of *ab initio* dipole moment surfaces (DMSs) is the systematic adoption of computed intensities in the place of measured ones for both water and CO_2 in the recent (2016) release of HITRAN [9]. The use of this methodology is particularly powerful for isotopically substituted species for which the accuracy of the computations is essentially unchanged [25–27], but experimental determinations become much harder. These studies employ the Lodi–Tennyson method [28] which uses stability analysis based on calculations using two different PESs and two different DMSs to identify 'unstable' transitions for which the computed intensities are not reliable. Significant differences between intensities calculated using different PESs for certain transitions have been found for water [27,29], CO_2 [30] and H_2CO [31]. Conversely, for many transitions it has proved possible to compute the line intensities for water [29,32] and CO_2 [33] with sub-per cent accuracy, which reflects the accuracy of the underlying *ab initio* DMS. To make further progress on this problem, it becomes important to estimate and eliminate the causes of the remaining uncertainties. The largest of these appears to be the calculation of wave functions for states which are affected by accidental interactions with other states of the same overall symmetry; spectroscopers generally call these interactions resonances. It is the failure to precisely treat these resonances that leads to the unstable transitions. As shown below, better treatment can be achieved by systematic improvement of the PES and hence the wave functions.

Section 2 describes the procedure used to obtain our new PES. Section 3 presents the computed energy levels obtained using our new PES. Section 4 compares and discusses calculations of intensities using different PESs. Section 5 describes our new, room temperature $H_2{}^{16}O$ line list. Section 6 presents our conclusions and plans for further work.

2. New potential energy surface

As a starting point for the optimization process, we used a semi-empirical PES due to Bubukina *et al.* [21]. Bubukina *et al.*, in turn, used the high-quality CVRQD *ab initio* PES [34,35] as their starting point and augmented this surface with corrections for adiabatic [36], relativistic [37] and quantum electrodynamics [38] effects. This fully *ab initio* starting point predicts rotation–vibration energy levels with an accuracy of about $1\,\mathrm{cm}^{-1}$.

(a) Nuclear motion calculation

Variational nuclear motion calculations were performed in Radau coordinates using DVR3D [39]. Morse-like oscillators with the values of parameters $r_e = 2.55$, $D_e = 0.25$ and $\omega_e = 0.007$ in atomic units were used for both radial coordinates, and associated Legendre functions for the angular coordinate as basis functions. The corresponding discrete variable representation grids contained 29, 29 and 40 points for these coordinates, respectively. The final diagonalized vibrational matrices had a dimension of 1500. For the rotational problem, the dimensions of final matrices can be obtained as $400(J + 1 - p)$, where J is the total angular momentum quantum number and p is the value of parity. Only nuclear masses were used in these calculations. To ensure good accuracy for high-J calculations, we followed the approach of Bubukina *et al.* [21] to rotational non-adiabatic effects which adopts a simplification [40] of *ab initio* procedure developed by Schwenke [41] for treating non-Born–Oppenhemer effects. The values of the adjustable parameters used by Bubukina *et al.* to scale Schwenke's results were left unchanged.

(b) Optimization results

The optimization procedure was based on a method developed by Yurchenko *et al.* [42].

This method allows the fit to simultaneously optimize reproduction of empirical energy levels and *ab initio* grid points. This procedure helps the fit to avoid nonphysical behaviour in the optimized PES. For this purpose, we used a set of 677 *ab initio* energies computed by Grechko *et al.* [43] in the energy region up to 25 000 cm^{-1} (approx. 2.7% of *ab initio* points from the original set of 696 energies were excluded from the fit).

In the fit, we varied the values of 240 potential parameters of the starting PES to obtain the best predicts of the most-accurate available empirical energy levels [24]. As a result, we obtain a potential which reproduces the set of 847 empirical energy levels with J values 0, 2 and 5, and lying below 15 000 cm^{-1} with a standard deviation of 0.011 cm^{-1}. The initial fit had the *ab initio* grid points weighted at 10^{-4} in the empirical data to ensure that PES remained physical, i.e. did not develop holes, in the region of interest. For the final stages of the fit, this weighting was reduced to 10^{-8}. Approximately 3% of energy levels from the complete empirical set in the energy region of interest (26 from the total set of 873 energies) were excluded from the fit. Most of these levels (approx. 20) have high values of bending quantum number v_2 and sample a region of the potential which is not well characterized by fit. The standard deviation of our final PES with respect to the set of Born–Oppenheimer *ab initio* points is about 68.8 cm^{-1}, a figure which depends strongly on high energy points.

Because the PES is designed for studies of states up to 15 000 cm^{-1}, we refer to it as PES15k below. A Fortran program giving the PES15k potential is given in the electronic supplementary material.

3. Results of the energy level calculations

Table 1 presents results of a $J = 0$ calculations using PES15k.

Table 2 presents results of a comparison of the standard deviations for states with rotational quantum numbers J up to 15 and lying below 15 000 cm^{-1} using the PES of Bubukina *et al.* [21] and PES15k. These standard deviations are computed from the discrepancies between calculated and experimental levels as follows. Empirical energy levels up to $J = 15$ were taken from the recent IUPAC compilation [24,44]. Not all the levels were included for the comparison. Some of the levels—approximately 2% of those derived in [24]—were excluded as they were outliers. There are two reasons that certain levels might show larger discrepancies. First, it could be the genuine experimental inaccuracy or incorrectly incorporated data. A number of problems with the IUPAC compilation of energy levels have been identified and are in the processes of being fixed [45]. Second, our model becomes worse for very highly excited v_2 bending vibrational quantum numbers and correspondingly for very highly excited K_a rotational quantum numbers.

Table 1. Observed vibrational band origins below 15 000 cm^{-1} calculated with the new PES; values are in cm^{-1}.

$v_1v_2v_3$	obs	calc	obs−calc	$v_1v_2v_3$	obs	calc	obs−calc
0 1 0	1594.7463	1594.7523	0.0060	0 0 1	3755.9285	3755.9277	−0.0009
0 2 0	3151.6298	3151.6453	0.0155	0 1 1	5331.2673	5331.2658	−0.0015
1 0 0	3657.0533	3657.0406	−0.0126	0 2 1	6871.5202	6871.5225	0.0023
0 3 0	4666.7905	4666.7948	0.0043	1 0 1	7249.8169	7249.8175	0.0006
1 1 0	5234.9756	5234.9759	0.0004	0 3 1	8373.8514	8373.8529	0.0015
0 4 0	6134.0150	6134.0207	0.0057	1 1 1	8806.9990	8806.9972	−0.0018
1 2 0	6775.0935	6775.0906	−0.0029	0 4 1	9833.5829	9833.5805	−0.0025
2 0 0	7201.5399	7201.5414	0.0016	1 2 1	10328.7293	10328.7248	−0.0044
0 0 2	7445.0562	7445.0269	−0.0293	2 0 1	10613.3563	10613.3510	−0.0053
0 5 0	7542.3725	7542.4207	0.0482	0 0 3	11032.4041	11032.3939	−0.0102
1 3 0	8273.9757	8273.9713	−0.0044	0 5 1	11242.7757	11242.7716	−0.0041
2 1 0	8761.5816	8761.5851	0.0035	1 3 1	11813.2069	11813.2046	−0.0023
0 1 2	9000.1360	9000.1258	−0.0103	2 1 1	12151.2539	12151.2438	−0.0101
2 2 0	10284.3644	10284.3588	−0.0055	0 1 3	12565.0064	12564.9970	−0.0094
0 2 2	10521.7577	10521.7435	−0.0142	1 4 1	13256.1550	13256.1584	0.0034
3 0 0	10599.6860	10599.6789	−0.0071	2 2 1	13652.6532	13652.6523	−0.0009
1 0 2	10868.8747	10868.8608	−0.0139	3 0 1	13830.9368	13830.9336	−0.0032
2 3 0	11767.3890	11767.3673	−0.0217	0 2 3	14066.1936	14066.1769	−0.0167
0 3 2	12007.7743	12007.7778	0.0034	1 0 3	14318.8121	14318.8008	−0.0113
3 1 0	12139.3153	12139.3065	−0.0088	1 5 1	14647.9733	14647.9996	0.0263
1 1 2	12407.6620	12407.6465	−0.0155				
3 2 0	13640.7166	13640.6811	−0.0355				
4 0 0	13828.2747	13828.2615	−0.0132				
1 2 2	13910.8936	13910.8796	−0.0140				
2 0 2	14221.1585	14221.1459	−0.0126				
0 0 4	14537.5043	14537.4859	−0.0184				

There are particular issues with quantum numbers of high v_2 states [46] and transitions to these states are, in general, much weaker than the other transitions, thus the influence of such lines on the accuracy of any line list is minor. As we can see from table 2, the improved average accuracy, expressed in the form of the standard deviation, varies between a factor of 1.5 and 2, which is significant.

4. Comparison of intensities

The intensity of a transition depends upon the square of the transition dipole. The transition dipole between two states can be computed using the following expression:

$$\mu_{\mathrm{if}} = \sum_t < i|\mu_t|f >, \tag{4.1}$$

where for a vibration–rotation transition, the initial and final states are represented by nuclear motion wave functions $|i>$ and $|f>$, and the sum runs over the components of the internal dipole

Table 2. Standard deviation, in cm^{-1}, as a function of rotational excitation, J, of $H_2{}^{16}O$ energy levels obtained from calculations with two PESs with respect to the empirical energy levels [24]; N gives the number of levels considered for each J.

J	N	Bubukina *et al.* [21]	PES15k
0	41	0.0145	0.0108
1	148	0.0181	0.0116
2	249	0.0239	0.0110
3	356	0.0186	0.0109
4	450	0.0166	0.0101
5	548	0.0174	0.0092
6	623	0.0169	0.0104
7	663	0.0162	0.0111
8	682	0.0238	0.0153
9	662	0.0257	0.0188
10	610	0.0280	0.0215
11	586	0.0328	0.0260
12	545	0.0400	0.0288
13	495	0.0432	0.0313
14	441	0.0483	0.0335
15	387	0.0491	0.0347

moment vector, $\underline{\mu}$. For a given DMS, differences in the values of the intensities reflect differences in the wave functions obtained as a result of the solution of the nuclear-motion Schrödinger equation for a certain PES. In this work, all calculations use the LTP2011 DMS of Lodi *et al.* [32], which is the most accurate DMS currently available.

The steady improvement in intensity measurements [33,47–50,50,51] towards the sub-per cent level of accuracy has paralleled attempts to improve the accuracy of intensity calculations. Given an accurate, *ab initio* DMS [32,33], the Lodi–Tennyson method [28] tests for unstable transitions, whose intensities cannot be determined accurately. These transitions are identified on the basis of four line list calculations using two PESs and two DMSs. The usefulness of the Lodi–Tennyson method depends strongly on the accuracy of both the primary PES and the secondary PES. For example, attempts to use an *ab initio* PES as a secondary PES normally result in a significant overestimation of number of unstable lines [30]. Thus, we need extremely accurate PESs for at least three reasons. The first is determination of the most accurate line positions in the calculation of molecular line lists. The second is for accurate wave functions which can be used for the accurate intensity calculations. The third is that an excellent pair of PESs are necessary for the Lodi–Tennyson-style evaluation of stability.

For these purposes, it is important to evaluate what is the difference in intensity accuracy for the different lines using the same DMS and two different very accurate PESs. As is shown in the previous section, the accuracy of the PES of this work is extremely high, whereas the accuracy of the PES of Bubukina *et al.* [21] is also very high, and it becomes an interesting problem to compare the intensities coming from these two PESs. For this purpose, we computed the line list considering all transitions below $15\,000\,cm^{-1}$ involving states with up to $J = 4$ using these two PESs. Table 3 presents a comparison of the differences in intensities of resulting 8701 lines. It can be seen that for most of the lines, more than 75%, the transition intensity is essentially unchanged (changes by less than 0.1%) by the change wave functions, while approximately 1% of the lines change by more than 5%.

Table 3. Comparison of intensities computed using wave functions from the PES15k and Bubukina *et al.* [21]. The comparison is for 8686 transitions between states with $J \leq 4$. The percentage differences are computed as $100 \times (I(\text{PES15}) - I(\text{Bubukina}))/I(\text{PES15})$.

%	no. lines
≥20%	8
5–20%	73
2–5%	213
1–2%	292
0.2–0.5%	1090
≤0.1%	4974

Table 4. Sample comparison of intensity calculations for the region 3495–3500 cm^{-1}. Experimental measurements are taken from Loos *et al.* [29,52] and have uncertainties better than 1%. The predicted intensities used wave functions calculated using PES15k (this work) and the PES of Bubukina *et al.* [21].

frequency	assignment				I(exp)	I(PES15k)	I(Bubukina)	δI(PES15k) (%)	δI(Bubukina) (%)
3495.065	1 0 0	13 3 10	0 0 0	13 4 9	2.62(−25)	2.6063(−25)	2.6054(−25)	−0.45	−0.48
3495.176	1 0 0	6 2 5	0 0 0	7 1 6	1.62(−21)	1.6070(−21)	1.6086(−21)	−0.93	−0.83
3495.506	1 0 0	13 5 8	0 0 0	14 4 11	1.44(−25)	1.4901(−25)	1.4904(−25)	3.36	3.38
3496.164	1 1 0	2 1 2	0 1 0	3 2 1	1.51(−24)	1.4784(−24)	1.4776(−24)	−2.07	−2.12
3496.279	1 0 0	9 4 6	0 0 0	9 5 5	9.76(−24)	9.6424(−24)	9.6300(−24)	−1.25	−1.38
3496.383	1 0 0	11 5 6	0 0 0	12 4 9	6.21(−24)	6.1797(−24)	6.1846(−24)	−0.54	−0.46
3496.624	1 0 0	5 1 4	0 0 0	6 2 5	3.30(−21)	3.2581(−21)	3.2555(−21)	−1.28	−1.37
3496.917	1 0 0	11 7 5	0 0 0	12 6 6	3.73(−25)	3.7945(−25)	3.8019(−25)	1.75	1.94
3497.601	0 2 0	5 5 0	0 0 0	6 2 5	2.29(−23)	2.1521(−23)	2.4768(−23)	−6.27	7.66
3497.985	1 0 0	10 6 5	0 0 0	11 5 6	1.29(−23)	1.2870(−23)	1.2898(−23)	0.00	0.22
3498.602	0 0 1	6 3 4	0 0 0	6 5 1	6.70(−23)	6.6933(−23)	6.7045(−23)	−0.06	0.11
3499.420	1 1 0	6 3 4	0 1 0	6 4 3	1.58(−25)	1.5306(−25)	1.5297(−25)	−3.03	−3.09
3499.561	0 0 1	15 3 13	0 0 0	15 3 12	7.71(−26)	7.5541(−26)	7.5730(−26)	−2.00	−1.74
3499.746	0 0 1	8 5 3	0 0 0	9 5 4	7.79(−22)	7.8226(−22)	7.8306(−22)	0.47	0.57
3499.925	0 2 0	7 3 4	0 0 0	6 2 5	8.07(−23)	8.1491(−23)	8.1537(−23)	0.99	1.05

Table 4 presents an example of the calculation of intensities of water absorption lines in the small spectral region between 3495 cm^{-1} and 3500 cm^{-1} using wave functions calculated by two different PESs: PES15k (this work) and Bubukina *et al.* [21]. For many lines, the difference is less than 0.1%. Some of the lines intensities differ more significantly by approximately 0.2%. There are also a few lines with a significant difference in intensities of more than 1%. For one line, the difference is 13%; this line was previously deemed unstable using the Lodi–Tennyson method [29].

Figure 1 gives a similar comparison with the recent high-accuracy measurements of Sironneau & Hodges [50] who consider 70 unblended water lines in the transparency window region from 7710 cm^{-1} to 7920 cm^{-1}; the stated uncertainty of these measurements is only 0.20%. For most transitions, the difference between the predictions of calculations performed with wave

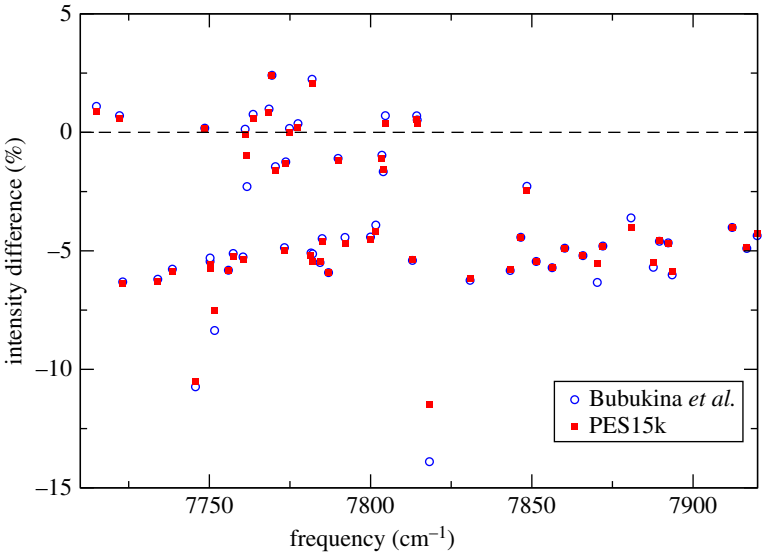

Figure 1. Differences, per cent of the observed value, for transition intensities predicted using wave functions from the PES15k and Bubukina *et al.* [21]. The observed data are taken from the recent high-accuracy measurements by Sironneau & Hodges [50]. (Online version in colour.)

functions from the PES15k and Bubukina *et al.* PESs is small. However, in general, our new calculations with PES15k give results closer to the measurements.

5. Line list calculation

Given the improved quality of the intensities generated with the new PES15k potential, we have computed a new room temperature line list for $H_2{}^{16}O$. The line list uses the PES15k PES and the LTP2011 DMS [32]. The line list includes all transitions with an intensity greater than 10^{29} cm molecule^{-1} at 296 K involving states with $J \leq 15$ and transition wavenumbers below 18 000 cm^{-1}. This line list, which follows the HITRAN convention that scales the intensities to natural abundance, contains 132 034 transitions. It is given in HITRAN format as part of the electronic supplementary material.

6. Conclusion

Since the pioneering work of Murrell and his group on the representation of PESs for polyatomic molecules, the story has been one of steady improvements. The best surfaces are now capable of giving predictions competitive with spectroscopic measurements [53]. Of course, a PES only exists within the Born–Oppenheimer approximation, so the generation of high-accuracy potentials necessarily brings beyond Born–Oppenheimer effects into play. How best to include these is a subject of active research for small molecules such as water [41,54,55].

There has been much recent emphasis on using highly accurate PES and *ab initio* DMS to compute transition intensities with accuracies approaching that achieved by many experimental studies. Understandably, much emphasis has been placed on *ab initio* techniques for computing high-accuracy DMS [32,56,57]. However, the PES used plays an important role in providing reliable wave functions; this is particularly important for those states which are sensitive to interactions with other nearby states of the same overall J and symmetry. In this work, we provide a new PES of improved accuracy which is used to provide a new $H_2{}^{16}O$ line list. We show that while for the majority of transitions the use of wave functions generated employing this new PES simply replicates results already available, for a minority of transitions, the use

of the new PES gives results which are significantly different and which generally represent an improvement.

Our analysis shows that for more than 10% of the lines, the use of our improved PES results in a change in the predicted intensity by more than 0.1%. Given that the most recent studies measure intensities for a few, carefully chosen $H_2{}^{16}O$ lines with an accuracy of 0.2% [50], improvements of this magnitude are important for the matching theoretical model. However, as is clear from the results presented above and from other published studies [29,58], the best currently available *ab initio* DMS is not able to provide this level of accuracy for many bands. Work on improving the accuracy and extending the range of DMS is currently in progress.

Data accessibility. Additional data for this article are given in the electronic supplementary material.

Competing interests. We declare we have no competing interests.

Funding. This work was supported by the UK Natural Environment Research Council through grant no. NE/N001508/ and the Russian Fund for Fundamental Studies (grant no. 15-02-07887).

Acknowledgements. We thank Sergey Yurchenko for helpful discussions during the course of this work.

References

1. Sorbie KS, Murrell JN. 1975 Analytical potentials for triatomic molecules from spectroscopic data. *Mol. Phys.* **29**, 1387–1407. (doi:10.1080/00268977500101221)
2. Murrell JN, Sorbie KS, Varandas AJC. 1976 Analytical potentials for triatomic molecules from spectroscopic data. *Mol. Phys.* **32**, 1359–1372. (doi:10.1080/00268977600102741)
3. Farantos S, Leisegang EC, Murrell JN, Sorbie K, Texeiradias JJC, Varandas AJC. 1977 Analytical potentials for triatomic molecules from spectroscopic data. *Mol. Phys.* **34**, 947–962. (doi:10.1080/00268977700102261)
4. Murrell JN, Carter S, Varandas AJC. 1978 Analytical potentials for triatomic molecules from spectroscopic data. *Mol. Phys.* **35**, 1325–1336. (doi:10.1080/00268977800100981)
5. Murrell JN, Carter S, Mills IM, Guest MF. 1979 Analytical potentials for triatomic molecules from spectroscopic data. *Mol. Phys.* **37**, 1199–1222. (doi:10.1080/00268977900100881)
6. Murrell JN, Carter S, Mills IM. 1979 Analytical potentials for triatomic molecules from spectroscopic data. *Mol. Phys.* **37**, 1885–1899. (doi:10.1080/00268977900101391)
7. Liu XH, Murrell JN. 1992 Analytical potential for HCP from spectroscopic data. *J. Chem. Soc., Faraday Trans.* **88**, 1503–1506. (doi:10.1039/ft9928801503)
8. Murrell JN, Carter S, Farantos SC, Huxley P, Varandas AJC. 1984 *Molecular potential energy functions*. Chichester, UK: John Wiley & Sons.
9. Gordon IE *et al.* 2017 The HITRAN2016 molecular spectroscopic database. *J. Quant. Spectrosc. Radiat. Transf.* **203**, 3–69. (doi:10.1016/j.jqsrt.2017.06.038)
10. Bernath PF. 2009 Molecular astronomy of cool stars and sub-stellar objects. *Int. Rev. Phys. Chem.* **28**, 681–709. (doi:10.1080/01442350903292442)
11. Murrell JN, Carter S, Mills IM, Guest MF. 1981 Analytical potentials for triatomic molecules. *Mol. Phys.* **42**, 605–627. (doi:10.1080/00268978100100491)
12. Carter S, Handy NC. 1987 A theoretical determination of the rovibrational energy levels of the water molecule. *J. Chem. Phys.* **87**, 4294–4301. (doi:10.1063/1.452887)
13. Halonen L, Carrington Jr T. 1988 Fermi resonances and local modes in water, hydrogen sulfide, and hydrogen selenide. *J. Chem. Phys.* **88**, 4171–4185. (doi:10.1063/1.453824)
14. Paulse CD, Tennyson J. 1994 An empirical potential energy surface for water accounting for states with high angular momentum. *J. Mol. Spectrosc.* **168**, 313–322. (doi:10.1006/jmsp.1994.1280)
15. Partridge H, Schwenke DW. 1997 The determination of an accurate isotope dependent potential energy surface for water from extensive *ab initio* calculations and experimental data. *J. Chem. Phys.* **106**, 4618–4639. (doi:10.1063/1.473987)
16. Yurchenko SN, Voronin BA, Tolchenov RN, Doss N, Naumenko OV, Thiel W, Tennyson J. 2008 Potential energy surface of HDO up to 25 000 cm^{-1}. *J. Chem. Phys.* **128**, 044312. (doi:10.1063/1.2806165)
17. Polyansky OL, Jensen P, Tennyson J. 1994 A spectroscopically determined potential energy surface for the ground state of $H_2{}^{16}O$: a new level of accuracy. *J. Chem. Phys.* **101**, 7651–7657. (doi:10.1063/1.468258)

18. Polyansky OL, Jensen P, Tennyson J. 1996 The potential energy surface of $H_2{}^{16}O$. *J. Chem. Phys.* **105**, 6490–6497. (doi:10.1063/1.472501)
19. Kain JS, Polyansky OL, Tennyson J. 2000 The ground-state potential energy surface of water: barrier to linearity and its effect on the vibration–rotation levels. *Chem. Phys. Lett.* **317**, 365–371. (doi:10.1016/S0009-2614(99)01389-5)
20. Shirin SV, Polyansky OL, Zobov NF, Ovsyannikov RI, Császár AG, Tennyson J. 2006 Spectroscopically determined potential energy surfaces of the $H_2{}^{16}O$, $H_2{}^{17}O$, and $H_2{}^{18}O$ isotopologues of water. *J. Mol. Spectrosc.* **236**, 216–223. (doi:10.1016/j.jms.2006.01.012)
21. Bubukina II, Polyansky OL, Zobov NF, Yurchenko SN. 2011 Optimized semiempirical potential energy surface for $H_2{}^{16}O$ up to 26 000 cm^{-1}. *Optics Spectrosc.* **110**, 160–166. (doi:10.1134/S0030400X11020032)
22. Polyansky OL, Zobov NF, Mizus II, Lodi L, Yurchenko SN, Tennyson J, Császár AG, Boyarkin OV. 2012 Global spectroscopy of the water monomer. *Phil. Trans. R. Soc. A* **370**, 2728–2748. (doi:10.1098/rsta.2011.0259)
23. Tennyson J, Zobov NF, Williamson R, Polyansky OL, Bernath PF. 2001 Experimental energy levels of the water molecule. *J. Phys. Chem. Ref. Data* **30**, 735–831. (doi:10.1063/1.1364517)
24. Tennyson J *et al.* 2013 IUPAC critical evaluation of the rotational–vibrational spectra of water vapor. Part III: energy levels and transition wavenumbers for $H_2{}^{16}O$. *J. Quant. Spectrosc. Radiat. Transf.* **117**, 29–58. (doi:10.1016/j.jqsrt.2012.10.002)
25. Zak EJ, Tennyson J, Polyansky OL, Lodi L, Zobov NF, Tashkun SA, Perevalov VI. 2017 Room temperature line lists for CO_2 symmetric isotopologues with *ab initio* computed intensities. *J. Quant. Spectrosc. Radiat. Transf.* **189**, 267–280. (doi:10.1016/j.jqsrt.2016.11.022)
26. Zak EJ, Tennyson J, Polyansky OL, Lodi L, Zobov NF, Tashkun SA, Perevalov VI. 2017 Room temperature linelists for CO_2 asymmetric isotopologues with *ab initio* computed intensities. *J. Quant. Spectrosc. Radiat. Transf.* **203**, 265–281. (doi:10.1016/j.jqsrt.2017.01.037)
27. Kyuberis AA, Zobov NF, Naumenko OV, Voronin BA, Polyansky OL, Lodi L, Liu A, Hu S-M, Tennyson J. 2017 Room temperature line lists for deuterated water. *J. Quant. Spectrosc. Radiat. Transf.* **203**, 175–185. (doi:10.1016/j.jqsrt.2017.06.026)
28. Lodi L, Tennyson J. 2012 Line lists for $H_2{}^{18}O$ and $H_2{}^{17}O$ based on empirical line positions and *ab initio* intensities. *J. Quant. Spectrosc. Radiat. Transf.* **113**, 850–858. (doi:10.1016/j.jqsrt.2012.02.023)
29. Birk M, Wagner G, Loos J, Lodi L, Polyansky OL, Kyuberis AA, Zobov NF, Tennyson J. 2017 Accurate line intensities for water transitions in the infrared: comparison of theory and experiment. *J. Quant. Spectrosc. Radiat. Transf.* **203**, 88–102. (doi:10.1016/j.jqsrt.2017.03.040)
30. Zak E, Tennyson J, Polyansky OL, Lodi L, Tashkun SA, Perevalov VI. 2016 A room temperature CO_2 line list with *ab initio* computed intensities. *J. Quant. Spectrosc. Radiat. Transf.* **177**, 31–42. (doi:10.1016/j.jqsrt.2015.12.022)
31. Al-Refaie AF, Yurchenko SN, Yachmenev A, Tennyson J. 2015 ExoMol line lists—VIII. A variationally computed line list for hot formaldehyde. *Mon. Not. R. Astron. Soc.* **448**, 1704–1714. (doi:10.1093/mnras/stv091)
32. Lodi L, Tennyson J, Polyansky OL. 2011 A global, high accuracy *ab initio* dipole moment surface for the electronic ground state of the water molecule. *J. Chem. Phys.* **135**, 034113. (doi:10.1063/1.3604934)
33. Polyansky OL, Bielska K, Ghysels M, Lodi L, Zobov NF, Hodges JT, Tennyson J. 2015 High-accuracy CO_2 line intensities determined from theory and experiment. *Phys. Rev. Lett.* **114**, 243001. (doi:10.1103/PhysRevLett.114.243001)
34. Polyansky OL, Császár AG, Shirin SV, Zobov NF, Barletta P, Tennyson J, Schwenke DW, Knowles PJ. 2003 High-accuracy *ab initio* rotation-vibration transitions for water. *Science* **299**, 539–542. (doi:10.1126/science.1079558)
35. Barletta P, Shirin SV, Zobov NF, Polyansky OL, Tennyson J, Valeev EF, Császár AG. 2006 CVRQD *ab initio* ground-state adiabatic potential energy surfaces for the water molecule. *J. Chem. Phys.* **125**, 204307. (doi:10.1063/1.2378766)
36. Tennyson J. 1996 A new algorithm for Hamiltonian matrix construction in electron–molecule collision calculations. *J. Phys. B: At. Mol. Opt. Phys.* **29**, 1817–1828. (doi:10.1088/0953-4075/29/9/024)

37. Quiney HM, Barletta P, Tarczay G, Császár AG, Polyansky OL, Tennyson J. 2001 Two-electron relativistic corrections to the potential energy surface and vibration–rotation levels of water. *Chem. Phys. Lett.* **344**, 413–420. (doi:10.1016/S0009-2614(01)00784-9)
38. Pyykkö P, Dyall KG, Császár AG, Tarczay G, Polyansky OL, Tennyson J. 2001 Estimation of Lamb-shift effects for molecules: application to the rotation–vibration spectra of water. *Phys. Rev. A* **63**, 024502. (doi:10.1103/PhysRevA.63.024502)
39. Tennyson J, Kostin MA, Barletta P, Harris GJ, Polyansky OL, Ramanlal J, Zobov NF. 2004 DVR3D: a program suite for the calculation of rotation–vibration spectra of triatomic molecules. *Comput. Phys. Commun.* **163**, 85–116. (doi:10.1016/j.cpc.2003.10.003)
40. Tennyson J, Barletta P, Kostin MA, Polyansky OL, Zobov NF. 2002 Ab initio rotation–vibration energy levels of triatomics to spectroscopic accuracy. *Spectrochim. Acta A* **58**, 663–672. (doi:10.1016/S1386-1425(01)00663-1)
41. Schwenke DW. 2003 New rovibrational kinetic energy operators using polyspherical coordinates for polyatomic molecules. *J. Chem. Phys.* **118**, 10 431–10 438. (doi:10.1063/1.1574013)
42. Yurchenko SN, Carvajal M, Jensen P, Herregodts F, Huet TR. 2003 Potential parameters of PH_3 obtained by simultaneous fitting of *ab initio* data and experimental vibrational band origins. *Chem. Phys.* **290**, 59–67. (doi:10.1016/S0301-0104(03)00098-3)
43. Grechko M *et al*. 2009 State-selective spectroscopy of water up to its first dissociation limit. *J. Chem. Phys.* **131**, 221105. (doi:10.1063/1.3273207)
44. Tennyson J *et al.* 2014 A database of water transitions from experiment and theory (IUPAC technical report). *Pure Appl. Chem.* **86**, 71–83. (doi:10.1515/pac-2014-5012)
45. Furtenbacher T, Tennyson J, Naumenko OV, Polyansky OL, Zobov NF, Császár AG. In preparation.
46. Child MS, Weston T, Tennyson J. 1999 Quantum monodromy in the spectrum of H_2O and other systems: new insight into the level structure of quasi-linear molecules. *Mol. Phys.* **96**, 371–379. (doi:10.1080/00268979909482971)
47. Hodges JT, Lisak D, Lavrentieva N, Bykov A, Sinitsa L, Tennyson J, Barber RJ, Tolchenov RN. 2008 Comparison between theoretical calculations and high-resolution measurements of pressure broadening for near-infrared water spectra. *J. Mol. Spectrosc.* **249**, 86–94. (doi:10.1016/j.jms.2008.02.022)
48. Wuebbeler G, Viquez GJP, Jousten K, Werhahn O, Elster C. 2011 Comparison and assessment of procedures for calculating the R(12) line strength of the $\nu_1 + 2\nu_2 + \nu_3$ band of CO_2. *J. Chem. Phys.* **135**, 204304. (doi:10.1063/1.3662134)
49. Ghysels M, Liu Q, Fleisher AJ, Hodges JT. 2017 A variable-temperature cavity ring-down spectrometer with application to line shape analysis of CO_2 spectra in the 1600 nm region. *Appl. Phys. B* **123**, 124. (doi:10.1007/s00340-017-6686-y)
50. Sironneau VT, Hodges JT. 2015 Line shapes, positions and intensities of water transitions near 1.28 µm. *J. Quant. Spectrosc. Radiat. Transf.* **152**, 1–15. (doi:10.1016/j.jqsrt.2014.10.020)
51. Odintsova T, Fasci E, Moretti L, Zak EJ, Polyansky OL, Tennyson J, Gianfrani L, Castrillo A. 2017 Highly accurate intensity factors of pure CO_2 lines near 2 µm. *J. Chem. Phys.* **146**, 244309. (doi:10.1063/1.4989925)
52. Loos J, Birk M, Wagner G. 2017 Measurement of air-broadening line shape parameters and temperature dependence parameters of H_2O lines in the spectral ranges 1850–2280 cm^{-1} and 2390–4000 cm^{-1}. *J. Quant. Spectrosc. Radiat. Transf.* **203**, 103–118. (doi:10.1016/j.jqsrt.2017.03.033)
53. Pavanello M *et al.* 2012 Precision measurements and computations of transition energies in rotationally cold triatomic hydrogen ions up to the midvisible spectral range. *Phys. Rev. Lett.* **108**, 023002. (doi:10.1103/PhysRevLett.108.023002)
54. Diniz LG, Mohallem JR, Alijah A, Pavanello M, Adamowicz L, Polyansky OL, Tennyson J. 2013 Vibrationally and rotationally nonadiabatic calculations on H_3^+ using coordinate-dependent vibrational and rotational masses. *Phys. Rev. A* **88**, 032506. (doi:10.1103/PhysRevA.88.032506)
55. Scherrer A, Agostini F, Sebastiani D, Gross EKU, Vuilleumier R. 2017 On the mass of atoms in molecules: beyond the Born-Oppenheimer approximation. *Phys. Rev. X* **7**, 031035. (doi:10.1103/PhysRevX.7.031035)

56. Lodi L *et al.* 2008 A new *ab initio* ground-state dipole moment surface for the water molecule. *J. Chem. Phys.* **128**, 044304. (doi:10.1063/1.2817606)
57. Schwenke DW, Partridge H. 2000 Convergence testing of the analytic representation of an *ab initio* dipole moment function for water: improved fitting yields improved intensities. *J. Chem. Phys.* **113**, 6592–6597. (doi:10.1063/1.1311392)
58. Lampel J *et al.* 2017 Detection of water vapour absorption around 363 nm in measured atmospheric absorption spectra and its effect on DOAS evaluations. *Atmos. Chem. Phys.* **17**, 1271–1295. (doi:10.5194/acp-17-1271-2017)